$\sigma = 1.74$. The boundary-layer quantities obtained numerically are given in Table 1 as compared with those from Eq. (9).

References

[1] Taylor, G. I., "The Boundary Layer in the Converging Nozzle of a Swirl Atomizer," *The Quarterly Journal of Mechanics and Applied Mathematics*, Vol. 3, Pt. 2, 1950, pp. 129–139.

[2] Cooke, J. C., "On Pohlhausen's Method with Application to a Swirl Problem of Taylor," *Journal of Aeronautical Sciences*, Vol. 19, No. 7, July 1952, pp. 486–490.

[3] Moore, F. K., "Three-Dimensional Boundary Layer Theory," *Advances in Applied Mechanics*, edited by H. L. Dryden and Tl. von Kármán, Vol. 4, Academic Press, New York, 1956, pp. 171–175.

[4] Mager, A., "Three-Dimensional Laminar Boundary Layers," *Theory of Laminar Flows*, edited by F. K. Moore, Princeton University Press, Princeton, N. J., 1964, pp. 321–328.

[5] Rott, N. and Lewellen, W. S., "Boundary Layers and Their Interactions in Rotating Flows," *Progress in Aeronautical Sciences*, edited by D. Küchemann, Vol. 7, Pergamon Press, Oxford, England, 1966, pp. 116–119.

[6] Gol'dshtik, M. A., "A Paradoxical Solution of the Navier-Stokes Equations," *Prikladnaia Matematika i Mekhanika* (English Translation), Vol. 24, No. 4, 1960, pp. 913–929.

[7] Kidd, G. J., Jr. and Farris, G. J., "Potential Vortex Flow Adjacent to a Stationary Surface," *Journal of Applied Mechanics*, Vol. 35, No. 2, June 1968, pp. 209–215.

[8] Schwiderski, E. W., "On the Axisymmetric Vortex Flow Over a Flat Surface," *Journal of Applied Mechanics*, Vol. 36, No. 3, Sept. 1969, pp. 614–619.

[9] Stuart, J. T., "On the Effects of Uniform Suction on the Steady Flow Due to a Rotating Disk," *The Quarterly Journal of Mechanics and Applied Mathematics*, Vol. 7, Pt. 4, 1954, pp. 446–457.

[10] Nachtsheim, P. R. and Swigert, P., "Satisfaction of Asymptotic Boundary Conditions in Numerical Solution of Systems of Nonlinear Equations of Boundary-Layer Type," TN D-3004, 1965, NASA.

Shock and Vibration Isolation Using a Nonlinear Elastic Suspension

T. E. Shoup*
Rutgers University, New Brunswick, N. J.

SHOCK and vibration problems in the aerospace and transportation industries arise from many causes, such as the isolation of instruments and controls or the protection of human occupants of vehicles. The usual solution to these problems involves the use of lightly damped flexible supports. These soft supports cause the natural frequency of the suspension system to be far below the disturbing frequency. This solution is effective for the isolation of steady-state vibration; however, when these suspensions encounter shock excitation their softness often leads to damagingly large deflections. It has been pointed out that this undesirable feature is not present in suspension systems utilizing symmetrically nonlinear springs that harden.[1–3] These springs become progressively stiffer when subjected to large deflections from their "operating point." A thorough discussion of analysis methods for systems having nonlinear springs has been made by Stoker.[4]

A number of ingenious ways have been developed to produce nonlinear spring devices,[5,6] but unfortunately many of these are not symmetrical in behavior or are rather complex to construct. As weight, cost, and reliability requirements become more important, designers are forced to search for new ways to improve existing designs by reducing the number of moving parts in suspension systems. Because of its simple construction and symmetrically hardening behavior, the device shown in Fig. 1a holds much promise as a shock and vibration isolation mount. The purpose of this Note is to present information for use in the design of suspension systems utilizing this device.

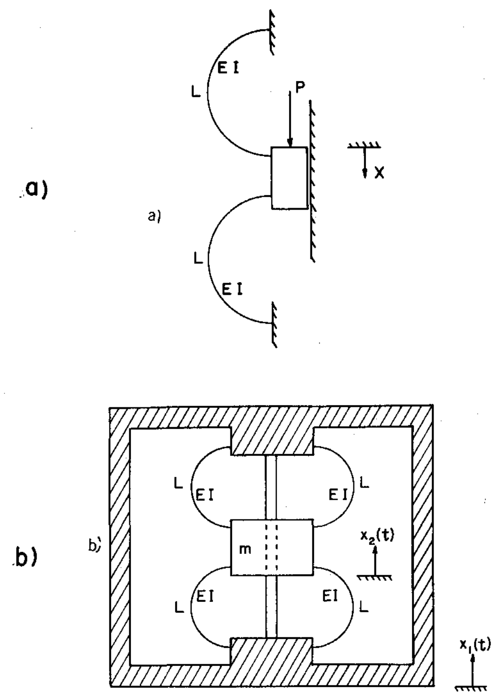

Fig. 1 The "elastica" suspension spring: a) single spring pair; b) two spring pairs in parallel.

Elastica Suspension Spring

The device shown in Fig. 1a consists of a pair of flexible strips each having length L, elastic modulus E, and cross section moment of inertia I. These two initially straight strips are each clamped in a semicircular shape. As the center platform is forced downward the upper flexible strip deflects into a shape called the "nodal elastica" and the lower strip deflects into a shape called the "undulating elastica." The describing equations for these "elastica" curves are well known[7]

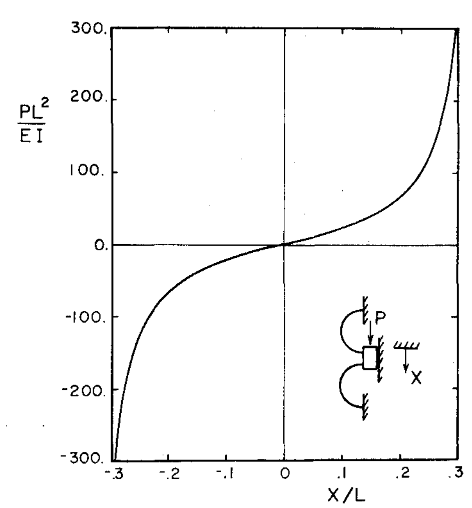

Fig. 2 Nondimensional load-vs-deflection curve for the "elastica" suspension spring pair.

Received February 11, 1971; revision received March 27, 1971. The author gratefully acknowledges the financial assistance given by the Rutgers University Research Council in support of this investigation.

* Assistant Professor of Mechanical and Aerospace Engineering.

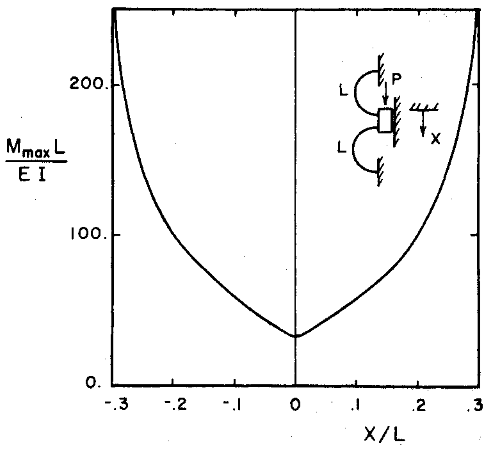

Fig. 3 Nondimensional maximum bending moment-vs-deflection curve for the "elastica" suspension spring pair.

and arise due to consideration of an exact expression of the moment-curvature relationship for the bending of beams. Utilizing these equations, the load-vs-deflection curve shown in Fig. 2 may be obtained. In this figure the plot is nondimensional for design purposes. A fundamental consideration in the selection of suspension springs is that of stress. The stress in the flexible strips is caused by the combined effects of bending and simple tension or compression. The bending stress will be maximum where the bending moment of the two strips is maximum. This critical point occurs where the curvature of the strips is maximum and its value can be determined from Fig. 3. The maximum bending moment will always occur in the strip deflected as the "nodal elastica." The total theoretical deflection of an elastica spring pair can never exceed $L(1 - 2/\pi)$ from its equilibrium position since this deflection corresponds to the configuration in which one of the strips is stretched perfectly straight. In actual practice this upper bound on deflection will not be achieved since the flexible strip in tension would undergo plastic deformation before reaching this theoretical maximum.

Flexible strips used as springs are often constructed with plate proportions since thin, wide cross sections permit large deflections at low bending stress levels. In this case, Figs. 2 and 3 can be utilized for design if the product EI is replaced by $EI/(1 - \nu^2)$ where ν is Poisson's ratio for the material being used.

It is sometimes convenient to use several identical elastica springs in parallel as shown in Fig. 1b. In this case, Figs. 2 and 3 would represent the behavior of each individual spring pair. The total load carried by a multiple pair system would be the sum of the loads carried by each elastica spring pair,

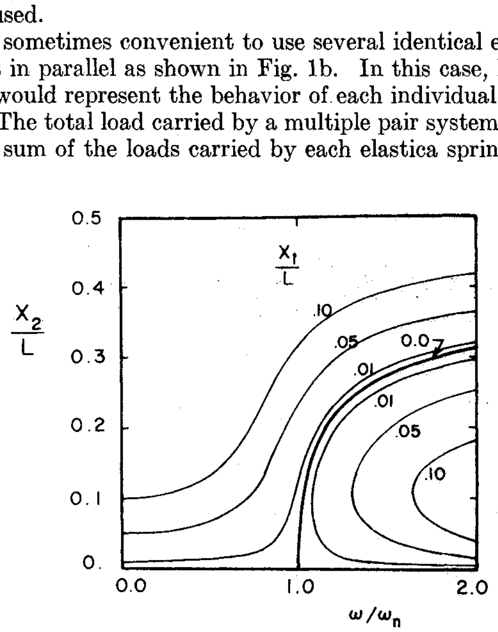

Fig. 4 Frequency response of the "elastica" suspension system.

and the maximum bending moment for each pair would be the same.

Suspension Dynamics

For a mass of m (lbm) supported on an elastica suspension system as shown in Fig. 1b the natural frequency for small deflections will be

$$\omega_n = 285.\ (EIn/L^3m)^{1/2} \qquad \text{(rad/sec)}$$

where E is the elastic modulus (psi), I is the moment of inertia (in.[4]), L is the length of each flexible strip, and n is the number of spring pairs in parallel. ($n = 2$ for Fig. 1b). Since elastic springs are doubly clamped beams, they possess a beam natural frequency apart from the suspension dynamics. Elastica springs will not perform as desired when the frequency of suspension motion is near to the beam natural frequency. If a suspension system as shown in Fig. 1b is subjected to a displacement $x_1(t) = X_1 \sin\omega t$ the resulting motion $x_2(t)$ of the suspended platform will be approximately sinusoidal and will be somewhat distorted for large values of the relative displacement $x_2(t) - x_1(t)$. If the output motion is considered to be of the form $x_2(t) = X_2 \sin\omega t$, the Ritz Averaging Method[4] may be employed to determine the relationship between input and output motion.

The equation of motion for this system is

$$m\ddot{x}_1 + P[x_1(t) - x_2(t)] = 0$$

where $P[x_1(t) - x_2(t)]$ is the load as a function of displacement difference. The Ritz Averaging Method chooses the amplitude of the output motion X_2 so as to make the average value of the virtual work per cycle vanish:

$$0 = \int_0^\tau [-m\omega^2 X_1 \sin\omega t + P(X_1 \sin\omega t - X_2 \sin\omega t)] X_2 \sin\omega t \, dt$$

This integration was performed numerically on an IBM 1130 computer and the results are shown in Fig. 4. The natural frequency of free vibration for this suspension system is represented by the curve $X_1/L = 0$ and increases as the amplitude of the vibration increases. The response curves of Fig. 4 contain two branches for each X_1/L value. Branches to the left of the free response curve correspond to motion that is in phase with the input $x_2(t)$ whereas branches to the right of the free response curve correspond to motion that is 180° out of phase with the input. Figure 4 predicts three possible amplitude values for some values of ω/ω_n. Of these three, only the upper value (in phase motion) and the lowest value (lower value 180° out of phase) are physically realizable. Small amounts of damping would cause corresponding branch curves of Fig. 4 to cross the free response curve and join. For such a damped system, actual amplitude values will "jump" from one portion of the response curve to another portion whenever a vertical tangent to that curve exists. This amplitude "jump" for nonlinear systems is discussed in detail by Stoker.[4]

References

[1] Efstathiades, G. J. and Williams, C. J. H., "Vibration Isolation Using Non-Linear Springs," *International Journal of Mechanical Science*, Vol. 9, 1967, pp. 27–44.

[2] Tobias, S. A., "Design of Small Isolator Units for the Suppression of Low-Frequency Vibration," *Journal Mechanical Engineering Science*, Vol. 1, No. 3, 1959, pp. 280–292.

[3] Young, D., Barton, M. V., and Fung, Y. C., "Shock Spectra for Nonlinear Spring-Mass Systems and Their Applications to Design," *AIAA Journal*, Vol. 1, No. 7, July 1963, pp. 1597–1602.

[4] Stoker, J. J., *Nonlinear Vibrations*, Interscience, New York, 1950.

[5] Chironis, N. P., *Spring Design and Application*, McGraw-Hill, New York, 1965.

[6] Welch, W. A., "These New Methods Simplify Design of Nonlinear Springs," *Product Engineering*, Vol. 36, No. 2, Oct. 11, 1965, pp. 138–141.
[7] Frisch-Fay, R., *Flexible Bars*, Butterworth, London, England, 1962.
[8] Timoshenko, S., *Vibration Problems in Engineering*, Van Nostrand, New York, 1955.

Underexpanded Jets of Liquid-Gas Bubble Mixtures

Armand Gosselin* and S. C. Kranc†
School of Engineering Science, Florida State University, Tallahassee, Fla.

Nomenclature

D = nozzle diameter
L = cell length
P_a = ambient pressure
P_o = stagnation pressure
P^* = static pressure in throat at choking
δ = concentration (volume of gas to volume of liquid)
θ = jet angle

THE speed of a low-frequency pressure pulse traveling in a liquid suspension of gas bubbles is known to be quite low due to the combination of the high compressibility and density of the mixture.[1] For example, the speed of a pulse traveling in a 50% volumetric concentration of air bubbles in water at atmospheric pressure is about 65 fps. Because of this fact it is easy to produce compressible supersonic flows of these mixtures in the laboratory as was shown in an early experiment by Tangren, Dodge and Seifert.[1] A subsequent study by Campbell and Pitcher[2] demonstrated the existence of shock-like regions of rapid bubble compression. Miur and Eichorn[3] extended the experimental work of Tangren et al. to a two-dimensional convergent-divergent nozzle and in a recent work, Eddington[4] constructed and tested a continuous flow tunnel and examined flow over wedge bodies.

The purpose of this Note is to discuss the free expansion of a bubbly flow. In Ref. 1 it was observed that a water-air bubble mixture broke up into a spray when exhausting to atmospheric pressure at supersonic velocities. In a study reported here it was found that a continuous jet having a structure similar to an underexpanded gas jet exiting from a convergent nozzle is also possible under some conditions. This mode of jet structure has apparently not been observed previously for these mixtures.

A suspension of fine air bubbles in glycerine was formed by high-speed mechanical mixing. A small amount (6 g/liter) of sodium lauryl sulphate was added to the glycerine to obtain higher bubble concentrations. The density of the mixture was measured directly from the weight of a known volume. A freejet was produced in a blow-down type facility by accelerating the mixture through a $\frac{1}{4}$-in. nozzle from an upstream reservoir at atmospheric pressure into an evacuated chamber.

Tests were run at various pressure ratios for several gas concentrations. Typical results are shown in Fig. 1 for a volumetric ratio of gas to liquid $\delta = 0.45$. For this concentration of air in glycerin, calculations based on Ref. 1 indicate that the jet is choked for pressure ratios above $P^*/P_o = 0.455$. Choking was confirmed in independent measurements of flow rate and static pressure at the throat.

Received March 15, 1971; revision received April 22, 1971.
Index Categories: Multiphase Flows; Jets, Wakes, and Viscid-Inviscid Flow Interactions.
* Research Assistant.
† Assistant Professor. Associate Member AIAA.

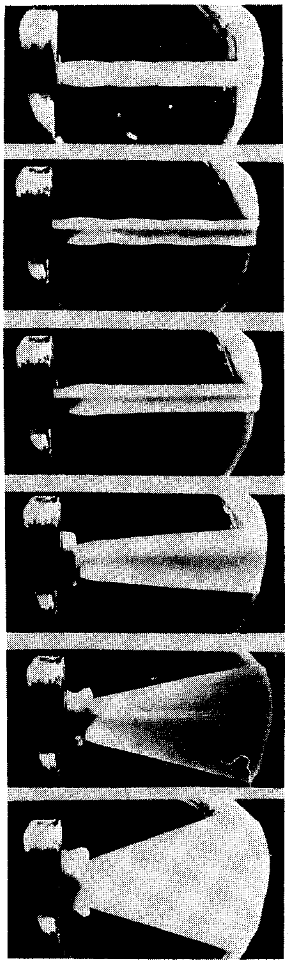

Fig. 1 Jet structure at various pressure ratios ($\delta_0 = 0.45$).

The photographs show that for pressure ratios above choking the jet develops a cell-like periodic structure which increases in size as the pressure ratio is increased. Figure 2 shows the increase in cell size at a relatively low gas concentration as a function of ambient pressure above critical ($P^* - P_a/P_o$). At higher concentration such as those shown in the photograph, the increase in cell size is considerably less. Qualitatively this behavior is analogous to the supersonic

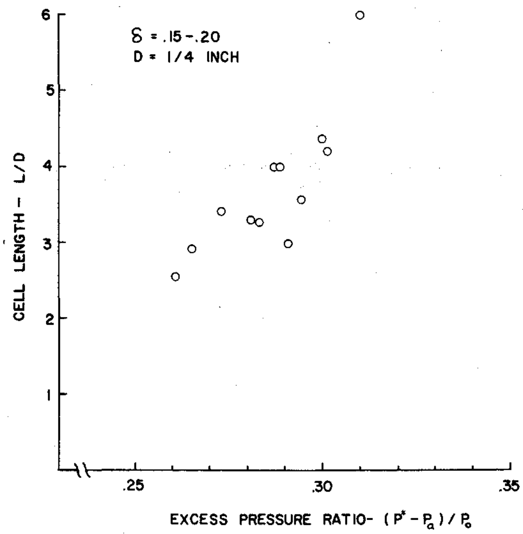

Fig. 2 Cell dimensions for continuous jet.